J Math Chem (2015) 53:629–650
DOI 10.1007/s10910-014-0445-7

ORIGINAL PAPER

On the cluster structure of linear-chain fermionic wave functions

Josef Paldus · Tokuei Sako · Geerd H. F. Diercksen

Received: 13 November 2014 / Accepted: 25 November 2014 / Published online: 6 December 2014
© Springer International Publishing Switzerland 2014

Abstract Using the model of cyclic polyenes C_NH_N with a nondegenerate ground state, $N = 4\nu + 2$ ($\nu = 1, 2, \ldots$), as a prototype of extended linear metallic-like systems we explore the cluster structure of the relevant wave functions. Based on the existing configuration interaction and coupled cluster (CC) results, as obtained with the Hubbard and Pariser–Parr–Pople Hamiltonians in the entire range of the coupling constant extending from the uncorrelated Hückel limit to the fully correlated limit, we recall the breakdown of the CCD or CCSD methods as the size of the system increases and the strongly correlated regime is approached. We introduce the concept of the indecomposable quadruply-excited clusters which arise for $\nu > 1$ and represent those connected quadruples that do not possess any corresponding disconnected cluster component. It is shown via explicit enumeration that the ratio of the number of these

J. Paldus (✉)
Department of Applied Mathematics, University of Waterloo, Waterloo, ON N2L 3G1, Canada
e-mail: paldus@uwaterloo.ca
URL: http://www.math.uwaterloo.ca/~paldus/

J. Paldus
Department of Chemistry, Guelph-Waterloo Center for Graduate Work in Chemistry $(GWC)^2$ - Waterloo Campus, University of Waterloo, Waterloo, ON N2L 3G1, Canada

T. Sako
Laboratory of Physics, College of Science and Technology, Nihon University, 7-24-1 Narashinodai, Funabashi, Chiba 274-8501, Japan
e-mail: sako@phys.ge.cst.nihon-u.ac.jp
URL: http://www.phys.ge.cst.nihon-u.ac.jp/~sako/

G. H. F. Diercksen
Max-Planck-Institut für Astrophysik, Karl-Schwarzschild-Strasse 1, 85741 Garching, Germany
e-mail: ghd@mpa-garching.mpg.de
URL: http://www.mpa-garching.mpg.de/mol_physics/index.shtml

indecomposables relative to that of the decomposables depends linearly on the size of the polyene N, so that the limit of the ratio of the number of indecomposables relative to the total number of quadruples approaches unity as $N \to \infty$. We then briefly outline the implications of these results for the applicability of CC approaches to extended systems and provide a qualitative argument for an even more extreme behavior of hexa-excited, octa-excited, etc., clusters as $N \to \infty$.

Keywords Linear chain models · Cyclic polyenes · Coupled cluster approach (CCA) · Cluster analysis · Decomposable and indecomposable connected quadruples · CCA to extended linear fermionic chains

Mathematics Subject Classification 81Q05 · 81Q80 · 81V55 · 81V70 · 92E10

1 Introduction

Quantum chemical methods that are based on the coupled cluster (CC) Ansatz for the wave function represent nowadays often used, highly accurate and reliable approaches to the electronic structure of molecular systems (see, e.g., [1–7]; for a historical overview, see [8,9]). This is particularly the case for closed-shell (CS), non-degenerate ground states where the single reference (SR) CC methods have been successfully applied, even though much progress was also made in handling of quasi-degenerate and open-shell (OS) systems, including excited states, by relying on multi-reference (MR) CC approaches (see, e.g., [10]). Nonetheless, the exploitation of CC Ansätze for quasi-degenerate or highly-degenerate states is far from being settled.

The correlation problem is particularly challenging for one-dimensional (1D) extended systems, such as found in metallic-like linear chains. The restriction to one dimension was initially employed for the sake of simplicity, as in the case of the pioneering work of Bethe [11] on the Heisenberg model [12] of a linear chain of spin-$\frac{1}{2}$ particles, which introduced what is nowadays referred to as the Bethe Ansatz. Seven years later this effort was extended by Hulthén [13], who considered the ground state of an antiferromagnetic case of the Heisenberg model, while relying on Bethe's Ansatz. However, this Ansatz (also referred to as the Bethe-Hulthén scheme; for a nice brief overview of these developments see, e.g., [14]) was not revived until a quarter of a century later for the 1D model of interacting spinless bosons [15] and five years later for the fermionic case, where one has to account for the spin-degree of freedom, requiring a generalization to the nested Bethe Ansatz [16]. The latter was also crucial for the handling of the Hubbard lattice model of electrons with short-range on-site interaction via Lieb–Wu equations [17,18]. The 1D fermionic problem then led to a formulation of the Yang–Baxter equations [16,19], which opened the way to the wealth of applications in statistical mechanics and solid-state physics, ranging from superconductivity and neutron scattering to quantum entanglement, quantum field theory, as well as to the introduction of quantum groups and string theory. Very recently it is also providing a testing ground for a realization of various models for the trapping of atoms in optical lattices [20]. There exists nowadays a very rich literature on these topics, including various review papers [14,21] and monographs (see, e.g., [22–30]).

An excellent model example of such 1D extended systems is provided by the so-called cyclic polyenes $C_N H_N$, $N = 2n = 4\nu + 2, \quad \nu = 1, 2, 3, \ldots$, when $\nu \to \infty$. These systems have a nondegenerate CS ground state and may also be regarded as linear metals with Born-von Kármán cyclic boundary conditions. When described by semi-empirical Hamiltonians, such as the Hubbard or Pariser–Parr–Pople (PPP) Hamiltonian, one can in fact vary the degree of quasi-degeneracy by varying the coupling constant via the scaling of the resonance (or hopping) integral β characterizing its one-electron component (see below). In this way we can achieve a continuous transition from a non-degenerate, uncorrelated case ($\beta \to \infty$) to a degenerate, completely correlated state ($\beta = 0$). Moreover, when relying on the Hubbard Hamiltonian, the geometry of these systems is irrelevant. Another great advantage of the Hubbard Hamiltonian description is the possibility to compare the CC energies with the exact ones obtained by solving the pertinent Lieb-Wu equations [31,32] (see also the Appendix to [33]). Unfortunately, the corresponding wave functions that are based on the Bethe Ansatz are not easily accessible to analysis. Yet, the dependence of the Hubbard correlation energies on the coupling constant is qualitatively the same as that obtained with the more realistic PPP Hamiltonian. For these reasons the cyclic polyene model was widely studied using various approaches accounting for the correlation effects (see, e.g., [34–42] and references therein).

The SR CC approaches—even when truncated to only doubles (i.e., CCD, which is in this case equivalent to CCSD)—work reasonably well for small finite polyenes away from the fully correlated limit (i.e., for small coupling constants or large β values), while their performance rapidly deteriorates when approaching the fully correlated limit. For example, for the PPP model of the smallest $N = 6$ polyene (i.e., the benzene molecule) the error in the CCD energy[1] for the spectroscopic value of the resonance integral ($\beta \approx -2.4$ eV) amounts only to about 3 %, yet it rapidly increases to about 80 % in the fully correlated limit ($\beta = 0$). For the next $N = 10$ polyene, this error at $\beta = 0$ amounts already to about 1,000 % and for the $N = 14$ ring CCD breaks down completely at about $\beta \approx -1.75$ eV (-1.37 eV for the Hubbard model) before reaching the fully correlated limit [34]. Extending CCD to CCDTQ ($\equiv$ CCSDTQ) helps to some extent, yet the same difficulties as found with CCD remain and are only shifted to larger cycles or larger coupling constants [43].

As is well known, the main reason for the success of the SR CC methods is the fact that for non-degenerate systems the quadruply-excited configurations are reasonably well approximated by their disconnected components given by the products of corresponding pair clusters. In the language of the CC formalism, the exact wave function is represented in the exponential form, $|\Psi\rangle = \exp(T)|\Phi\rangle$, with $|\Phi\rangle$ representing an independent particle model (IPM) wave function, most often realized by a Hartree-Fock (HF) wave function. The cluster operator T is then given by the sum of one-, two-, three-, etc., up to the N-body components, $T = \sum_{i=1}^{N} T_i$, so that, symbolically, we can describe the above mentioned property as $T_4 \ll \frac{1}{2} T_2^2$. Nonetheless, the impor-

[1] Note that in view of the high symmetry of cyclic polyenes all singly-excited clusters vanish so that CCD is equivalent with CCSD.

tance of connected quadruply-excited amplitudes constituting T_4 increases with the increasing quasi-degeneracy.

Now, already for the $N = 10$ polyene we find an interesting phenomenon, namely the existence of connected quadruples that have no corresponding disconnected counterpart, as first pointed out in the context of the cluster analysis of its full configuration interaction (FCI) wave function [44]. We shall refer to such quadruples as *indecomposable* ones in order to distinguish them from their *decomposable* counterparts that possess the corresponding disconnected quadruply-excited component given by the product of relevant pair clusters. We shall see that this phenomenon arises thanks to a high symmetry of our models and cannot arise in asymmetric systems.

In view of the fact that cyclic polyenes may be regarded as a model of linear metals, it is of interest to explore the relative importance of indecomposable and decomposable clusters, particularly in the $N \to \infty$ limit, as manifested by the trend in their relative occurrences. For example, designating the number of quadruples for the $N = 4\nu + 2$ polyene by $Q(N)$ and, similarly, the number of decomposable and indecomposable quadruples by $Q^{\mathrm{dec}}(N)$ and $Q^{\mathrm{indec}}(N)$, respectively, it would be of interest to find out how these quantities depend on the size of the polyene N and, in particular, to determine the limits like

$$\lim_{N\to\infty} \frac{Q^{\mathrm{indec}}(N)}{Q(N)} \quad \text{or} \quad \lim_{N\to\infty} \frac{Q^{\mathrm{indec}}(N)}{Q^{\mathrm{dec}}(N)}. \tag{1}$$

This information should help us to better understand the cluster structure of the corresponding wave functions and enable us to assess the capability of CC approaches to describe this type of systems. For large values of N we can also expect the importance of higher than quadruples and a similar behavior of their decomposable and indecomposable components.

2 Basic notation

Unlike the ab initio approaches that rely on nonorthogonal atomic orbitals (AOs) to define a truncated finite-dimensional Hilbert space employed, the semi-empirical approaches utilize a minimum basis set of hypothetical orthonormal AOs. We can thus employ the standard second quantization formalism associated with these basis sets as in the case of molecular orbitals (MOs) given as linear combinations of AOs. We shall label AOs by lower case Greek letters, e.g., $|\mu\rangle$, $|\nu\rangle$, etc., and MOs by the lower case letters of the Latin alphabet, e.g., $|a\rangle$, $|b\rangle$, etc., designating generic MOs by $|i\rangle$, $|j\rangle$, etc. The corresponding spin-orbitals, given by a simple product of an orbital and a spin function $|\sigma\rangle$, $\sigma = \pm\frac{1}{2}$, will then be designated by the corresponding capitals, e.g., $|M\rangle = |\mu\rangle|\sigma\rangle$ or $|A\rangle = |a\rangle|\sigma\rangle$. The corresponding creation and annihilation operators are then designated as $X_A^\dagger \equiv X_{a\sigma}^\dagger$ and $X_A \equiv X_{a\sigma}$, respectively. We also define the orbital unitary group, U(N), generators E_{ij} as (see, e.g., [45,46])

$$E_{ij} = \sum_\sigma X_{i\sigma}^\dagger X_{j\sigma}, \tag{2}$$

so that we can express the relevant spin-independent electronic Hamiltonian involving at most two-body interactions

$$H = \sum_i z_i + \sum_{i<j} v_{ij}, \tag{3}$$

in the following second-quantized form

$$\begin{aligned} H &= \sum_{i,j} \langle i|z|j\rangle \sum_\sigma X^\dagger_{i\sigma} X_{j\sigma} + \frac{1}{2} \sum_{i,j,k,l} \langle ij|v|kl\rangle \sum_{\sigma,\tau} X^\dagger_{i\sigma} X^\dagger_{j\tau} X_{l\tau} X_{k\sigma} \\ &= \sum_{i,j} \langle i|z|j\rangle E_{ij} + \frac{1}{2} \sum_{i,j,k,l} \langle ij|v|kl\rangle \left(E_{ik}E_{jl} - \delta_{jk}E_{il}\right), \end{aligned} \tag{4}$$

with i, j, k, l representing either the effective, hypothetical AOs μ, ν, etc., or MOs a, b, c, etc., either set being orthonormal.

3 Semiempirical π-eletron Hamiltonians

The π-eletron systems can be conveniently described by the semi-empirical Hamiltonian H_π of the PPP type (see, e.g., Sec. VI of [45])

$$H_\pi = \sum_{\mu,\nu} z_{\mu\nu} E_{\mu\nu} + \frac{1}{2} \sum_{\mu,\nu} \gamma_{\mu\nu} \left(E_{\mu\mu}E_{\nu\nu} - \delta_{\mu\nu}E_{\mu\nu}\right), \tag{5}$$

with indices $\mu, \nu = 1, 2, \ldots, N$ labeling the atomic sites and the AO unitary group generators $E_{\mu\nu}$ defined as in Eq. (2). Like any π-electron semi-empirical Hamiltonian, it is defined directly by specifying the one- and two-electron parameters $z_{\mu\nu}$ and $\gamma_{\mu\nu}$, respectively, rather than by selecting some actual spin orbital basis set as is the case of ab initio model Hamiltonians. For the two-center Coulomb-type two-electron integrals one invokes the zero differential overlap approximation [47], so that only the Coulomb-type integrals $\gamma_{\mu\nu} \equiv \langle \mu(1)\nu(2)|r_{12}^{-1}|\mu(1)\nu(2)\rangle$ are required.

The diagonal one-electron parameters $z_{\mu\mu}$ are approximated by relying on the Goeppert-Mayer and Sklar approximation (see, e.g., [47])

$$z_{\mu\mu} = \alpha_\mu - \sum_{\nu\neq\mu} Z_\nu \gamma_{\mu\nu}, \tag{6}$$

where α_μ is the so-called Coulomb integral (usually approximated by the valence state ionization potential) and Z_μ designates the number of π-electrons contributed by the μ-th atomic site. For the one-electron off-diagonal parameters $z_{\mu\nu}$ ($\mu \neq \nu$) one invokes the tight-binding approximation, so that in view of the D_{Nh} (or simply C_N) point group symmetry of our models (see Sec. 4 below) we can write

$$z_{\mu,\mu\pm1} = \beta \quad \text{and} \quad z_{\mu\nu} = 0 \ \text{ otherwise}, \tag{7}$$

with all indices taken modulo N.

When we include the internuclear repulsion term $\sum_{\mu<\nu} Z_\mu Z_\nu \gamma_{\mu\nu}$, we can thus rewrite the Hamiltonian (5) as follows

$$H_\pi = \sum_\mu \alpha_\mu + \sum_{\mu\nu}{}' \beta E_{\mu\nu} + \sum_{\mu<\nu} \gamma_{\mu\nu} \left(E_{\mu\mu} - Z_\mu\right)\left(E_{\nu\nu} - Z_\nu\right) + \frac{1}{2}\sum_\mu \gamma_{\mu\mu} E_{\mu\mu}\left(E_{\mu\mu} - 1\right), \tag{8}$$

where the prime on the second summation symbol implies the sum over nearest neighbors only. For cyclic polyenes each atomic site contributes only one electron ($Z_\mu = 1$) and all one-center Coulomb integrals are equivalent, so that

$$\alpha_\mu = \alpha_1 = 0 \quad \text{and} \quad \gamma_{\mu\mu} = \gamma_{11}, \tag{9}$$

with $\alpha_1 = 0$ defining the origin of the energy scale. Thus, finally, for the case of cyclic polyenes we can write the Hamiltonian (5) or (8) in a simple form (see, e.g., Eq. (6.19) of [45])

$$H_\pi = \beta \sum_\mu \left(E_{\mu,\mu+1} + E^\dagger_{\mu,\mu+1}\right) + \frac{1}{2}\sum_{\mu,\nu} \gamma_{\mu\nu}(n_\mu - 1)(n_\nu - 1), \tag{10}$$

where we designated the μth site occupation number operator by $n_\mu \equiv E_{\mu\mu}$.

The one-electron part of H_π is thus proportional to the resonance integral β whose reciprocal value can be viewed as a coupling constant, so that by varying β from zero to large negative values (in practice -5 or -10 eV) we can explore the whole range of the correlation effects from the fully or strongly correlated limit to the weakly or uncorrelated limit, respectively. We note that the strongly or fully correlated limit ($\beta \to 0$) corresponds to the strong coupling or a low density regime ($r_s \to \infty$) in the parlance of the electron-gas model and, similarly, the weakly correlated limit ($|\beta| \to \infty$) corresponds to the high-density limit ($r_s \to 0$). The physical (spectroscopic) value of β for the standard Coulomb integral approximations amounts to about -2.4 or -2.5 eV.

Various approximations are used for the two-electron Coulomb repulsion parameters $\gamma_{\mu\nu}$, the most common one for the PPP Hamiltonian being the Mataga–Nishimoto parametrization [48], i.e., a modified point charge approximation

$$\gamma_{\mu\nu} = e^2/(R_{\mu\nu} + c), \quad c = e^2/\gamma_{00}, \tag{11}$$

with one center integral $\gamma_{00} \equiv \gamma_{\mu\mu}$ given by the so-called I–A approximation [47] (for the PPP Hamiltonian $\gamma_{00} = 10.84$ eV) and $R_{\mu\nu}$ designating the internuclear separation between the atomic sites μ and ν (with the nearest neighbor site separation taken as 1.4 Å). The geometry of the model implies that $\gamma_{\mu\nu} = \gamma_{\mu+\kappa,\nu+\kappa} = \gamma_{0,\mu-\nu}$.

In the Hubbard Hamiltonian only the on-site interactions are allowed, so that $\gamma_{\mu\nu} = \gamma\delta_{\mu\nu}$, with $\gamma = 5$ eV, roughly corresponding to the difference $(\gamma_{00} - \gamma_{01})$ in the PPP model [49]. In solid state texts the resonance integral β is referred to as the

hopping integral $t = |\beta|$ and the on-site repulsion integral $\gamma_{11} \equiv \gamma$ is designated by U. The relevant parameter defining the correlation strength is thus U/β. As already mentioned, the actual geometry of the model is irrelevant in this case since only the on-site Coulomb integral γ and the nearest-neighbor hopping term β play the role.

4 Cyclic polyene model

As already pointed out above the π-electron cyclic polyene model is useful when exploring the correlation effects in one-dimensional systems. The limiting case of infinitely large polyenes may then be regarded as a model of polyenic chains and the same model may also be thought of as a model of a linear metal with Born-von Kármán cyclic boundary conditions. In fact, this model is essentially equivalent to the model of an electron in a box with suitable boundary conditions [50–52].

Our hypothetical systems thus represent a π-electron model of cyclic polyenes $C_N H_N$ having a non-degenerate ground state ($N = 2n = 4\nu + 2,\ \nu = 1, 2, \ldots$) with carbon atomic sites located at the vertices of a regular N-gon. In view of the Bloch theorem the MOs $|a\rangle$, $a = 0, 1, 2, \ldots, (N-1)$, are completely determined by the symmetry of the system

$$|a\rangle = \left(1/\sqrt{N}\right) \sum_{\mu=0}^{N-1} \exp\left(i\omega a\mu\right)|\mu\rangle, \qquad \omega = 2\pi/N. \tag{12}$$

The one- and two-electron matrix elements of the Hamiltonian take a very simple form in the MO basis, namely (cf. [34])

$$\begin{aligned} \langle a|z|b\rangle &= 2\beta\delta_{ab}\cos(\omega a), \\ \langle ab|v|cd\rangle &= K(a-c)\delta_{a+b,c+d}, \end{aligned} \tag{13}$$

where

$$\begin{aligned} K(a) = K(-a) &= N^{-1} \sum_{\mu=0}^{N-1} \gamma_{0\mu} \exp(i\omega a\mu) \\ &= N^{-1} \left[\gamma_{00} + (-1)^a \gamma_{0n} + 2 \sum_{\mu=1}^{n-1} \gamma_{0\mu} \cos(\mu a\omega) \right], \end{aligned} \tag{14}$$

with all indices or arguments taken modulo N.

In order to distinguish MOs that are defining a CS ground-state IPM wave function, referred to as the occupied MOs, from the virtual or unoccupied ones, we shall label the former ones by the subscripted and the latter ones by the superscripted indices, i.e., as a_1, a_2, etc., and a^1, a^2, etc., respectively. The Hartree-Fock orbital energies ϵ_a are then

$$\epsilon_a = \langle a|f|b\rangle\delta_{ab} = 2\beta\cos(\omega a) + NK(0) - \sum_{a_1} K(a - a_1), \tag{15}$$

with the summation extending over the occupied (or hole) MOs a_1 ($-\nu \leq a_1 \leq \nu$) defining the HF sea. We note that the Bloch MOs (12) are pairwise degenerate, $\epsilon_a = \epsilon_{-a} \equiv \epsilon_{N-a}$, except when $a = 0$ or $a = n$.

The expressions for the one-and two-electron matrix elements of the Hamiltonian H_π and for the orbital energies take on a particularly simple form when we rely on the Hubbard Hamiltonian. Since only on-site Coulomb integrals are involved, the actual geometry of the molecular framework is irrelevant, just as in the case of the Hückel Hamiltonian. Thus, the quantities $K(a)$ are independent of the orbital label,

$$K(a) \equiv K = \gamma/N, \tag{16}$$

and the orbital energies are essentially those of the Hückel model, i.e.,

$$\epsilon_a = 2\beta \cos(\omega a) + \frac{1}{2}\gamma \tag{17}$$

5 Coupled cluster method

In contrast to the linear SR configuration interaction (CI) Ansatz for the exact wave function $|\Psi\rangle$,

$$|\Psi\rangle = \sum_{i=0}^{N} C_i |\Phi\rangle, \quad C_0 \equiv \hat{1}, \tag{18}$$

the SR CC method relies on the exponential Ansatz

$$|\Psi\rangle = \exp\Big(\sum_{i=0}^{N} T_i\Big)|\Phi\rangle, \tag{19}$$

where $|\Phi\rangle$ designates a single-determinantal IPM (usually HF) wave function. We employ the intermediate normalization $\langle\Psi|\Phi\rangle = 1$ in both cases. The CI and CC i-body operators C_i and $T_i (i = 1, 2, \ldots, N)$, respectively, are expressed as linear combinations of i-body excitation operators $G_i(\Omega)$ with coefficients representing the corresponding CI and CC amplitudes $c_j^{(i)}$ and $t_j^{(i)}$,

$$C_i = \sum_j c_j^{(i)} G_i(\Omega_j) \quad \text{and} \quad T_i = \sum_j t_j^{(i)} G_i(\Omega_j). \tag{20}$$

Labeling the spin orbitals $|A\rangle$ that are occupied and unoccupied in the reference IPM wave function $|\Phi\rangle$ by the subscripted and superscripted labels A_k and A^k, respectively, the excitation operators $G_i(\Omega_j)$ are given by

$$G_i(\Omega_j) = \prod_{k=1}^{i} (X_{A^k}^{\dagger} X_{A_k}), \quad \Omega_j \equiv \Big\{ A_k, A^k | k = 1, \ldots, i \Big\}. \tag{21}$$

The CI and CC operators C_i and T_i are then related as follows

$$C_i = T_i + \sum_{\lambda \vdash i} \prod_j \left(n_j!\right)^{-1} T_j^{n_j}, \tag{22}$$

where the summation extends over all nontrivial partitions λ of $i, \lambda \vdash i$, as given by the solutions of the Diophantine equation $i = \sum_{j=1}^{i-1} j n_j$. Here T_i's represent the connected cluster components, while the product terms on the right hand side of (22) represent the disconnected components. When Brueckner MOs are employed, the $C_1 = T_1$ components vanish, so that the first disconnected component appears in the quadruply-excited C_4, $C_4 = T_4 + \frac{1}{2} T_2^2$.

The main benefit of the exponential cluster Ansatz (19) stems from the possibility of an efficient truncation of the wave function expansion based on the linked cluster theorem of the many-body perturbation theory (MBPT) [53]. In this way the higher-excited components may be effectively approximated—at least for nonmetallic systems—by their disconnected components that arise automatically in the CC formalism via the exponential Ansatz. Specifically, since the singly-excited clusters T_1 usually play a secondary role (contributing only in higher orders of MBPT) and can be completely eliminated by relying on the maximum overlap (or Brueckner) MOs, the most important role is played by the pair cluster amplitudes $t_j^{(2)}$ constituting the doubly-excited component T_2 (doubles for short). Thus, setting $T \approx T_2$ we automatically account for quadruples by their disconnected component $\frac{1}{2} T_2^2$, yielding the so-called CCD method, which generally provides a very good description of the correlation effects. A small, yet often important connected triple (T_3) contribution is then usually accounted for perturbatively via the CCSD(T) approximation [54,55].

When deriving the explicit form of CC equations [56–59] (for a historical account see [8] and references therein) it is convenient to employ the normal product (N-product) form of the Hamiltonian (cf. [60]) relative to the IPM wave function $|\Phi\rangle$ as a Fermi vacuum for the hole–particle (h–p) second-quantized formalism, i.e.,

$$\begin{aligned} H_N &\equiv H - \langle \Phi | H | \Phi \rangle \\ &= \sum_{A,B} \langle A | f | B \rangle N \left[X_A^\dagger X_B \right] + \frac{1}{4} \sum_{A,B,C,D} \langle AB | v | CD \rangle_{\mathcal{A}} N \left[X_A^\dagger X_B^\dagger X_D X_C \right], \end{aligned} \tag{23}$$

where $\langle AB | v | CD \rangle_{\mathcal{A}}$ designates the antisymmetrized two-body matrix element

$$\langle AB | v | CD \rangle_{\mathcal{A}} \equiv \langle AB | v | CD \rangle - \langle AB | v | DC \rangle, \tag{24}$$

and $\langle A | f | B \rangle$ are the one-body IPM (usually HF) matrix elements

$$\langle A | f | B \rangle \equiv \langle A | z | B \rangle + \sum_{C_1} \langle AC_1 | v | BC_1 \rangle_{\mathcal{A}}. \tag{25}$$

This facilitates the exploitation of Wick's theorem and of Feynman-like diagrams while relying on the h-p formalism (see, e.g., [60]) and of the spin-angular-momentum

diagrams (see, e.g., [61]) when deriving the spin-adapted version of the CC formalism (see, e.g., [62]). Note that the excitation operators G_i are automatically in the N-product form since they involve only creation h-p operators.

Since the variational determination of cluster amplitudes leads to a very cumbersome formalism one relies on the Schrödinger equation $H_N|\Psi\rangle = \Delta\epsilon|\Psi\rangle$ projected onto the manifold of relevant excited configuration state functions (CSFs). Here $\Delta\epsilon \equiv E - \langle\Phi|H|\Phi\rangle$ designates the exact energy relative to the IPM model (i.e., the correlation energy when we use a HF reference). Thus, substituting the Ansatz (19) into the Schrödinger equation and exploiting the connected cluster theorem, i.e., $H_N \exp(T)|\Phi\rangle = \exp(T)[H_N \exp(T)]_{\mathcal{C}}|\Phi\rangle$, we obtain (see, e.g., [56–59])

$$\left(\left[H_N \exp(T)\right]_{\mathcal{C}} - \Delta\epsilon\right)|\Phi\rangle = 0, \tag{26}$$

where the subscript $\mathcal{C}$ indicates the connected part of the expression. By relying on the diagrammatic technique (or symbol manipulation codes) one can then obtain an explicit form of the above equation as a set of nonlinear algebraic equations for the unknown cluster amplitudes.

We must emphasize here that the actual values of the cluster amplitudes $t_j^{(i)}$ and thus of the operator T_i are well defined only in the context of the exact (i.e., FCI) wave function $|\Psi\rangle$. Otherwise, their values will depend on the approximation (i.e., the degree of truncation) employed. In fact, while they are always well defined relative to the exact $|\Psi\rangle$, they may be undefined in cases when the CC equations do not possess any real solution, as will be seen below.

The spin orbital form of the Hamiltonian, Eq. (23), is primarily employed in handling of OS systems (yet, often also for CS systems) when relying on the unrestricted HF (UHF) reference $|\Phi\rangle$, thus ignoring the spin-free nature of the molecular Hamiltonian and unnecessarily increasing the dimension of the problem. In the CS case, when $|\Phi\rangle$ is represented by a single Slater determinant with doubly occupied MOs, one can simply achieve the spin adaptation by assigning a factor of two to each closed loop of oriented lines in the resulting diagrams [56,57]. Nonetheless, such a formalism is based on nonorthogonal CSFs and once going beyond the doubles will involve more cluster amplitudes than necessary (see the discussion in [59]). The orthogonally spin-adapted version of the CCD method (referred to at the time as the coupled-pair many-electron theory CPMET) was presented in [62] and further developed in [63,64] (see also [65–67] and references therein). Yet another, a totally different spin-adapted version, may be obtained via the cluster Ansatz based on the unitary group approach (UGA-CC) [68,69].

6 Nature of many-body wave functions

As stated by Thouless [70] "the wave function of a many-body system is so complicated that any approximation to it will be almost orthogonal to it". In order to get some idea of these complexities we shall rely on earlier studies of cyclic polyenes $C_N H_N$ representing typical extended systems when $N \to \infty$. In fact, some of the characteristics of the relevant wave functions may be gleaned by examining those describing finite

Table 1 Contribution of doubles (D), triples (T), quadruples (Q), and higher than quadruples (>Q) to the FCI correlation energy of the PPP $N = 10$ cyclic polyene model (in %) and the difference R of the CCD and CIDQ energies relative to the FCI energy, $R \equiv (\Delta\epsilon^{(\mathrm{CCD})} - \Delta\epsilon^{(\mathrm{CIDQ})})/\Delta\epsilon^{(\mathrm{FCI})}$ (in %), as a function of the resonance integral β (in eV)

$-\beta$	D	T	Q	>Q	R
5.0	94.8	1.2	3.9	0.1	0.2
4.0	92.4	1.7	5.8	0.2	0.4
3.0	87.5	2.6	9.3	0.6	1.3
2.5	83.4	3.3	12.2	1.1	2.9
2.0	77.7	3.9	16.1	2.4	7.2
1.5	69.7	3.9	21.5	5.0	26.5
1.0	59.5	2.8	26.6	11.1	608.6
0.5	51.0	0.8	31.2	17.0	897.0
0.0	42.8	0.1	32.3	24.8	837.9

polyenes or chains while gradually increasing their size.[2] Moreover, the parametrization of the semi-empirical Hamiltonians defining these models enables us to vary the quasidegeneracy over the whole range of the coupling constant, as pointed out above. Since even here the corresponding wave functions are rather complex, most of the studies focussed on the correlation energies. Yet, we can draw some conclusions about the importance of various wave function components from limited CI and CC results.

The FCI and limited CI results and their CC structure were investigated in a considerable detail for the $N = 6$ and $N = 10$ rings using both the Hubbard and the PPP Hamiltonians [44]. The PPP FCI results were later extended to the $N = 14$ and $N = 18$ rings by Bendazzoli and Evangelisti [39] and Bendazzoli et al. [40] (see also [41,42]). However, already for the $N = 18$ ring, both the dimension of the FCI problem ($\approx 73 \times 10^6$) and the increasing quasidegeneracy did not allow the authors to reach the fully-correlated limit and proceed beyond $\beta = -2.5\,\mathrm{eV}$.

The $N = 6$ and $N = 10$ results clearly revealed an overwhelming importance of doubles and a rapidly increasing role of quadruples as the fully correlated limit is approached (cf. Figs. 4 and 5 and Tables IV–VII of [44]). Moreover, already the $N = 10$ results (Table 1) indicate an increasing importance of higher than quadruples in this limit. Contribution of triples is not only very small relative to that of doubly- and quadruply-excited CSFs but—except for the highly correlated region—is also approximately additive (cf. Table VIII of [44]).

Interestingly enough, while the difficulty of obtaining the FCI results rapidly increases when approaching the fully correlated limit and the CC methods break down completely (even when accounting for connected quadruples [43]) for large enough N values, the handling of the fully correlated limit ($\beta = 0$) becomes easy in view of the fact that only the electrostatic component of the Hamiltonian plays a role here. Indeed, it is not difficult to show (see, e.g., [44]) that the exact correlation energy at $\beta = 0$ becomes

[2] This approach is often used even when considering spin chains; see, e.g., [13] or [71].

$$-\Delta\epsilon^{\mathrm{PPP}}(\beta=0)=n(2n-1)K(0)-2\sum_{i<j}^{(\mathrm{occ})}K(i-j)-\sum_{\mu<\nu}\gamma_{\mu\nu}, \tag{27}$$

for the PPP Hamiltonian, while an almost trivial result is obtained for the Hubbard Hamiltonian

$$-\Delta\epsilon^{\mathrm{H}}(\beta=0)=n^2K(0)=\left(\nu+\frac{1}{2}\right)\gamma_{11}=\frac{1}{4}N\gamma. \tag{28}$$

Of course, in the latter case we can generate the exact FCI energies for any value of the coupling constant and any N using Lieb–Wu equations [31,33]. Unfortunately, this approach (like any based on the Bethe Ansatz) does not provide us with any information about the cluster structure of the corresponding wave functions. It is, however, an important realization that the Hubbard and PPP results exhibit a parallel behavior, both as far as the role played by various excitation orders in their contribution to the correlation energy and their weight in the resulting wave functions.

In this regard it is of interest to note the role played by the reference configuration $|\Phi\rangle$ in the FCI wave function. As can be seen from the results given in Table IX of [44] and Table I of [40], listing the coefficients (or their squares) of the reference configuration $|\Phi\rangle$ in the normalized FCI wave function $|\Psi\rangle(\langle\Psi|\Psi\rangle=1)$, the HF (or Brueckner) IPM reference $|\Phi\rangle$ provides the exact result in the uncorrelated limit when $|\beta|\rightarrow\infty$, while its weight almost vanishes in the fully correlated limit. In fact, we see that with the increasing N this weight rapidly approaches zero, amounting to 0.0686, 0.0094, and 0.0013 for $N=6$, 10, and 14, respectively [40]. Clearly, as $N\rightarrow\infty$ this weight will vanish making the exact wave function orthogonal to $|\Phi\rangle$. In fact, this will also be the case when we choose a better reference than the IPM one (e.g., CID or CCD wave function), as the results of Table III of [40] clearly indicate. We recall here that since in the fully correlated limit the one-electron component of the Hamiltonian is absent, all excited CSFs become degenerate with the reference configuration. The above described behavior thus clearly indicates that in the fully correlated limit the cyclic polyene model represents a highly complex degenerate system.

Another aspect of the difficulties that we encounter when handling cyclic polyenes is revealed by the fact that with the increasing quasidegeneracy, the truncated CC equations may not possess any real valued, physically meaningful solution [34]. Thus, while at the CCD level we find real solutions in the whole range of the coupling constant for $N=6$ and $N=10$ (even though we encounter, respectively, a 100 and 1,000 % error in the correlation energy for $\beta=0$), no real solution exists for $N=14$ below certain critical value of $|\beta|$ (see [34] for details). This behavior persists even when one employs higher-level approximations, such as CC(S)DTQ [43]. This is clearly related with the growing importance of higher-excited cluster components as documented by the analysis given in [44]. As already alluded to in the Introduction, one interesting aspect that arises for larger and larger cycles is the existence of connected quadruples that have no corresponding disconnected conterparts, which we defined as the indecomposable quadruples. Clearly, such quadruples cannot be accounted for via their disconnected components, which is essential for the success of the CCD or CCSD approaches. We shall now turn our attention to this aspect.

7 Role of indecomposable quadruples

The cluster analysis of the FCI wave function for the first two cyclic polyenes $N = 6$ and $N = 10$ clearly indicates an increasing importance of connected quadruples as we approach the fully correlated limit (cf. Table 1 above and Table X and Figs. 8–11 of [44]). We again recall here a parallel behavior for the Hubbard and the PPP Hamiltonians, as well as the fact that the actual geometry of the model is irrelevant in the former case, where only topology plays a role (i.e., the adjacency in the tight-binding model). This parallel behavior is also revealed by the results for the correlation energy in larger polyenes (see, e.g., Fig. 5 of [34]).

Now, starting with the $N = 10$ ring we observe an interesting new phenomenon, which is clearly associated with the high symmetry of our models, namely that some of the connected quadruples do not possess corresponding disconnected counterparts given by the product of two doubles. We can thus refer to such quadruples as the *indecomposable* ones in contrast to the *decomposable* quadruples, which possess at least one disconnected counterpart. Of course, a similar situation will arise for even higher than quadruply-excited configurations, such as sextuples, octuples, etc. While no such indecomposable quadruple appears in the $N = 6$ case, we find already 22 of them for the $N = 10$ ring; they are listed in Table 2 (for simplicity's sake we ignore here the alternancy and hole-particle symmetries). Note that all these configurations correspond to one singlet CSF except for configurations 4 and 19 which involve four singly-occupied MOs and thus generate two singlet CSFs. Thus, the number of indecomposable CSFs for $N = 10$ equals 24, which will also be the number of corresponding indecomposable, connected, quadruply-excited cluster amplitudes.

We recall that we label the MOs by their quasimomentum k (or a), $k = 0, 1, \ldots, (N-1)$, Eq. (12), (see, e.g., Fig. 1 of [34] for a general schematic representation of Bloch orbital labeling and orbital energy distribution for $C_N H_N$). The ground state configuration $(0^2\, 1^2\, \ldots\, \nu^2\, (N-\nu)^2\, (N-\nu+1)^2\, \ldots\, (N-1)^2)$ or the corresponding CSF is then associated with a zero quasimomentum $k = 0 \,(\mathrm{mod}\, N)$, so that only CSFs belonging to the same irrep of C_N (i.e., having the same quasimo-

Table 2 Indecomposable quadruples for $N = 10$ cyclic polyene

i	$\lvert\Phi_i^{\mathrm{occ}\to\mathrm{unocc}}\rangle$	i	$\lvert\Phi_i^{\mathrm{occ}\to\mathrm{unocc}}\rangle$
1	$0^2\,2^2 \to 3^2\,4^2$	12	$2^2\,8^2 \to 3\,5\,6^2$
2	$0\,1^2\,2 \to 3^2\,4^2$	13	$2^2\,9^2 \to 3\,6^2\,7$
3	$1\,2^2\,9 \to 3^2\,4^2$	14	$2^2\,8^2 \to 4^2\,5\,7$
4	$0\,1\,2^2 \to 3^2\,4\,5$	15	$1^2\,2\,8 \to 4^2\,7^2$
5	$1^2\,2^2 \to 3^2\,4\,6$	16	$8^2\,9^2 \to 4\,6\,7^2$
6	$1^2\,2^2 \to 3^2\,5^2$	17	$8^2\,9^2 \to 5^2\,7^2$
7	$2\,8\,9^2 \to 3^2\,6^2$	18	$8^2\,9^2 \to 5\,6^2\,7$
8	$0\,1^2\,8 \to 3^2\,7^2$	19	$0\,8^2\,9 \to 5\,6\,7^2$
9	$0\,2\,9^2 \to 3^2\,7^2$	20	$0^2\,8^2 \to 6^2\,7^2$
10	$1^2\,2^2 \to 3\,4^2\,5$	21	$0\,8\,9^2 \to 6^2\,7^2$
11	$1^2\,8^2 \to 3\,4^2\,7$	22	$1\,8^2\,9 \to 6^2\,7^2$

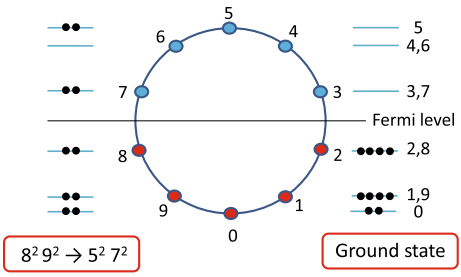

Fig. 1 A schematic representation of quadruple excitation $8^2\,9^2 \rightarrow 5^2\,7^2$ (or $1^2\,2^2 \rightarrow 3^2\,5^2$)

mentum $k = 0$) can interact with the ground state and thus appear in the pertinent wave function or CC formalism. Clearly, all singles are associated with a nonvanishing quasimomentum $k > 1$ and can be ignored. The number of singlet and triplet coupled doubles (the latter involving four distinct MO labels), $N_{S=0}^{(\mathrm{bi})}$ and $N_{S=1}^{(\mathrm{bi})}$, respectively, that are associated with a zero quasimomentum transfer (mod N) are given by

$$N_{S=0}^{(\mathrm{bi})} = \frac{4}{3}\nu(\nu^2+2) + 3\nu^2 + 1 \quad \text{and} \quad N_{S=1}^{(\mathrm{bi})} = \frac{2}{3}\nu(2\nu^2+1) + \nu^2\,. \tag{29}$$

Note that such configurations (CSFs or CC amplitudes) are simply generated by considering all possible pairs of, say, virtual MOs a^1, a^2 with occupied MOs given by $a_1 = a^1 - k$, $a_2 = a^2 + k$ yielding a zero quasimomentum transfer. Of course, here we require that $-\nu \leq a_i \leq \nu$, $i = 1, 2$ (all labels modulo N). We can then similarly generate possible zero quasimomentum transfer quadruples and check if there exists at least one possible pair of $k = 0$ doubles. In this way we can determine the number of decomposable and indecomposable quadruples for each polyene.

To provide an example of an indecomposable quadruple in the case of $N = 10$ polyene let us consider, for example, the excitation $8^2\,9^2 \rightarrow 5^2\,7^2$ (i.e., Φ_{17} in Table 2), shown schematically in Fig. 1. The ground state configuration ($0^2\,1^2\,2^2\,8^2\,9^2$) being associated with a zero quasimomentum [$k = 0\,(\mathrm{mod}N)$], only CSFs belonging to the same irrep of C_{10} (i.e., having the same quasimomentum $k = 0$) can interact with it and appear in the pertinent wave function or CC formalism. Considering now possible disconnected quadruples given by pairs of doubles, we find five possible candidates listed in Table 3, where we also parenthetically indicate the corresponding quasimomenta k for each double. We see that even though these pairs of doubles have zero quasimomentum, none of the individual doubles is associated with a zero quasimomentum. Consequently, none of these doubles can appear as a component of the ground state wave function and thus these disconnected quadruples will not play any role in the CC (in this case CCD) formalism.

We have developed appropriate codes that generate all relevant quadruples and analyze them for their decomposability. The resulting counts for the decomposable [$Q^{\mathrm{dec}}(N) \equiv D$] and indecomposable [$Q^{\mathrm{indec}}(N) \equiv I$] quadruples, as well as the number of all quadruples [$Q \equiv Q(N) = Q^{\mathrm{dec}}(N) + Q^{\mathrm{indec}}(N) = D + I$] are given in Table 4 for cyclic polyenes C_NH_N, $N = 4\nu + 2$ with $1 \leq \nu \leq 47$, where we also included the ratios $I/Q[\equiv Q^{\mathrm{indec}}(N)/Q(N)]$ and $I/D[\equiv Q^{\mathrm{indec}}(N)/Q^{\mathrm{dec}}(N)]$. The corresponding results for CSFs (accounting for a number of distinct singlets for

Table 3 Possible disconnected quadruples for the 17th configuration $8^2\,9^2 \rightarrow 5^2\,7^2$ of Table 2

i	$\lvert\Phi_i^{\text{occ}\rightarrow\text{unocc}}\rangle$	k	$\lvert\Phi_i^{\text{occ}\rightarrow\text{unocc}}\rangle$	k
1	$8^2 \rightarrow 7^2$	(-2)	$9^2 \rightarrow 5^2$	(2)
2	$8\,9 \rightarrow 5^2$	(-3)	$8\,9 \rightarrow 7^2$	(3)
3	$9^2 \rightarrow 7^2$	(-4)	$8^2 \rightarrow 5^2$	(4)
4	$8^2 \rightarrow 5\,7$	(-4)	$9^2 \rightarrow 5\,7$	(4)
5	$8\,9 \rightarrow 5\,7$	(±5)	$8\,9 \rightarrow 5\,7$	(±5)

configurations involving four or more distinct MOs) are then listed in Table 5. In each case we observe an initial rapid increase in the number of indecomposables $Q^{\text{indec}}(N)$ relative to the total number of quadruples $Q(N)$, as graphically illustrated in Fig. 2a.

Table 4 Number of all $[Q \equiv Q(N) = Q^{\text{dec}}(N) + Q^{\text{indec}}(N)]$, decomposable $[Q^{\text{dec}}(N) \equiv D]$, and indecomposable $[Q^{\text{indec}}(N) \equiv I]$ quadruple configurations and their ratios for cyclic polyenes C_NH_N, $N = 4\nu + 2$

ν	N	Orbital configurations			Ratios	
		$Q(N)$	$Q^{\text{dec}}(N)$	$Q^{\text{indec}}(N)$	Q^{indec}/Q	$Q^{\text{indec}}/Q^{\text{dec}}$
1	6	8	8	0	0.0000	0.0000
2	10	217	195	22	0.1014	0.1128
3	14	1927	1523	404	0.2096	0.2653
4	18	9852	6976	2876	0.2919	0.4123
5	22	36380	23432	12948	0.3559	0.5526
6	26	108361	64151	44210	0.4080	0.6892
7	30	277063	151935	125128	0.4516	0.8236
8	34	631840	322904	308936	0.4889	0.9567
9	38	1318088	630920	687168	0.5213	1.0891
10	42	2560161	1152651	1407510	0.5498	1.2211
11	46	4689759	1993283	2696476	0.5750	1.3528
12	50	8180364	3292848	4887516	0.5975	1.4843
13	54	13688428	5233224	8455204	0.6177	1.6157
14	58	22101793	8045751	14056042	0.6360	1.7470
15	62	34595919	12019495	22576424	0.6526	1.8783
16	66	52698656	17510152	35188504	0.6677	2.0096
17	70	78364008	24949600	53414408	0.6816	2.1409
18	74	114055465	34856067	79199398	0.6944	2.2722
19	78	162839671	47844971	114994700	0.7062	2.4035
20	82	228490844	64640376	163850468	0.7171	2.5348
21	86	315606524	86087096	229519428	0.7272	2.6661
22	90	429735449	113163439	316572010	0.7367	2.7975
23	94	577517943	146994599	430523344	0.7455	2.9288
24	98	766839392	188866664	577972728	0.7537	3.0602
25	102	1006997640	240241296	766756344	0.7614	3.1916

Table 4 continued

v	N	Orbital configurations			Ratios	
		$Q(N)$	$Q^{\mathrm{dec}}(N)$	$Q^{\mathrm{indec}}(N)$	Q^{indec}/Q	$Q^{\mathrm{indec}}/Q^{\mathrm{dec}}$
26	106	1308884657	302771027	1006113630	0.7687	3.3230
27	110	1685183055	378315203	1306867852	0.7755	3.4544
28	114	2150578316	468956568	1681621748	0.7819	3.5859
29	118	2721987052	577018496	2144968556	0.7880	3.7173
30	122	3418801873	705082839	2713719034	0.7938	3.8488
31	126	4263153759	856008447	3407145312	0.7992	3.9803
32	130	5280192224	1032950304	4247241920	0.8044	4.1118
33	134	6498383848	1239379312	5259004536	0.8093	4.2433
34	138	7949830105	1479102715	6470727390	0.8139	4.3748
35	142	9670604743	1756285171	7914319572	0.8184	4.5063
36	146	11701111292	2075470440	9625640852	0.8226	4.6378
37	150	14086461660	2441603744	11644857916	0.8267	4.7693
38	154	16876876041	2860054743	14016821298	0.8305	4.9009
39	158	20128104711	3336641159	16791463552	0.8342	5.0324
40	162	23901872704	3877653040	20024219664	0.8378	5.1640
41	166	28266347560	4489877672	23776469888	0.8412	5.2956
42	170	33296630721	5180625107	28116005614	0.8444	5.4271
43	174	39075273599	5957754363	33117519236	0.8475	5.5587
44	178	45692818476	6829700240	38863118236	0.8505	5.6903
45	182	53248364812	7805500784	45442864028	0.8534	5.8219
46	186	61850162017	8894825391	52955336626	0.8562	5.9535
47	190	71616228815	10108003559	61508225256	0.8589	6.0851

The observed trend seems to indicate that the ratio $Q^{\mathrm{indec}}(N)/Q(N) \equiv I/Q$ will approach unity as $N \to \infty$. This fact is then confirmed by considering the ratio of indecomposables relative to the decomposables $Q^{\mathrm{indec}}(N)/Q^{\mathrm{dec}}(N) \equiv I/D$ shown in Fig. 2b. This figure clearly implies a linear dependence of this ratio for large enough values of N, so that we can write that $I/D \sim N$ or, more precisely, that $I/D = cN - d$, with a small negative intercept $d > 0$. We can thus conjecture with great confidence that the sought after limits, Eq. (1), are given by

$$\lim_{N\to\infty} \frac{Q^{\mathrm{indec}}(N)}{Q^{\mathrm{dec}}(N)} = \lim_{N\to\infty} \frac{I}{D} \to \infty,$$

$$\lim_{N\to\infty} \frac{Q^{\mathrm{indec}}(N)}{Q(N)} = \lim_{N\to\infty} \frac{I}{Q} = \lim_{N\to\infty} \frac{N - d/c}{N - (d+1)/c} = 1. \tag{30}$$

Table 5 Number of all $[Q \equiv Q_0(N) = Q_0^{\mathrm{dec}}(N) + Q_0^{\mathrm{indec}}(N)]$, decomposable $[Q_0^{\mathrm{dec}}(N) \equiv D]$, and indecomposable $[Q_0^{\mathrm{indec}}(N) \equiv I]$ singlet quadruple configurations and their ratios for cyclic polyenes $C_N H_N$, $N = 4\nu + 2$

ν	N	SINGLET CONFIGURATIONS			RATIOS	
		$Q_0(N)$	$Q_0^{\mathrm{dec}}(N)$	$Q_0^{\mathrm{indec}}(N)$	Q_0^{indec}/Q_0	$Q_0^{\mathrm{indec}}/Q_0^{\mathrm{dec}}$
1	6	11	11	0	0.0000	0.0000
2	10	522	498	24	0.0460	0.0482
3	14	6587	5847	740	0.1123	0.1266
4	18	42472	35000	7472	0.1759	0.2135
5	22	185039	140727	44312	0.2395	0.3149
6	26	624122	438014	186108	0.2982	0.4249
7	30	1758183	1141235	616948	0.3509	0.5406
8	34	4333488	2610272	1723216	0.3976	0.6602
9	38	9635059	5405959	4229100	0.4389	0.7823
10	42	19737706	10353958	9383748	0.4754	0.9063
11	46	37825363	18617791	19207572	0.5078	1.0317
12	50	68586984	31781276	36805708	0.5366	1.1581
13	54	118697319	51939171	66758148	0.5624	1.2853
14	58	197390778	81797054	115593724	0.5856	1.4132
15	62	317136639	124780815	192355824	0.6065	1.5415
16	66	494423936	185154004	309269932	0.6255	1.6703
17	70	750664219	268144623	482519596	0.6428	1.7995
18	74	1113220442	380081610	733138832	0.6586	1.9289
19	78	1616570331	528538955	1088031376	0.6730	2.0586
20	82	2303612408	722489340	1581123068	0.6864	2.1884
21	86	3227122927	972467679	2254655248	0.6987	2.3185
22	90	4451372090	1290741938	3160630152	0.7100	2.4487
23	94	6053907703	1691493687	4362414016	0.7206	2.5790
24	98	8127514528	2191008632	5936505896	0.7304	2.7095
25	102	10782357715	2807874203	7974483512	0.7396	2.8400
26	106	14148318458	3563186954	10585131504	0.7482	2.9707
27	110	18377530131	4480770151	13896759980	0.7562	3.1014
28	114	23647123304	5587398064	18059725240	0.7637	3.2322
29	118	30162187767	6913030279	23249157488	0.7708	3.3631
30	122	38158959818	8491056278	29667903540	0.7775	3.4940
31	126	47908243231	10358546499	37549696732	0.7838	3.6250
32	130	59719072016	12556513496	47162558520	0.7897	3.7560
33	134	73942623227	15130183575	58812439652	0.7954	3.8871
34	138	90976388250	18129274558	72847113692	0.8007	4.0182
35	142	111268610667	21608283855	89660326812	0.8058	4.1493

Table 5 continued

ν	N	SINGLET CONFIGURATIONS			RATIOS	
		$Q_0(N)$	$Q_0^{\mathrm{dec}}(N)$	$Q_0^{\mathrm{indec}}(N)$	Q_0^{indec}/Q_0	$Q_0^{\mathrm{indec}}/Q_0^{\mathrm{dec}}$
36	146	135322998952	25626787092	109696211860	0.8106	4.2805
37	150	163703722447	30249742643	133453979804	0.8152	4.4117
38	154	197040698698	35547806550	161492892148	0.8196	4.5430
39	158	236035180407	41597658207	194437522200	0.8238	4.6742
40	162	281465650464	48482331596	232983318868	0.8277	4.8055
41	166	334194033123	56291557119	277902476004	0.8316	4.9368
42	170	395172229578	65122114274	330050115304	0.8352	5.0682
43	174	465448986419	75078189659	390370796760	0.8387	5.1995
44	178	546177105016	86271745652	459905359364	0.8420	5.3309
45	182	638621000087	98822900143	539798099944	0.8453	5.4623
46	186	744164615946	112860311242	631304304704	0.8483	5.5937
47	190	864319708463	128521572871	735798135592	0.8513	5.7251

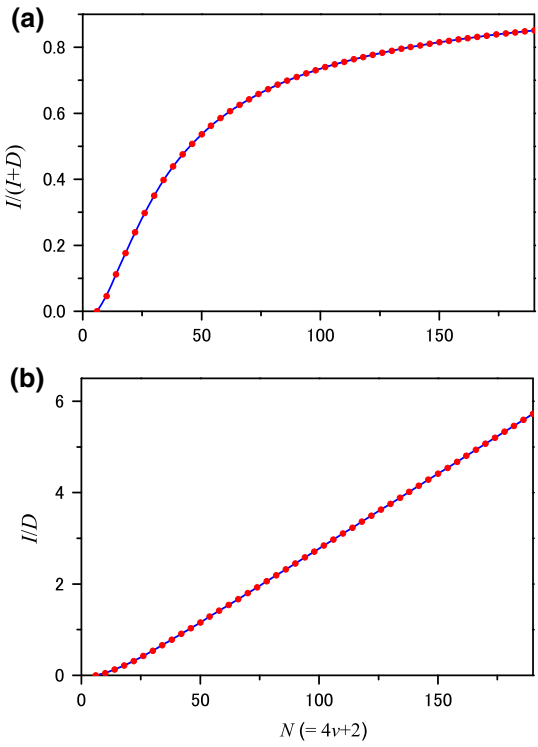

Fig. 2 **a** Dependence of the ratio $I/(D+I)$ of the number of indecomposable quadruples I to the total number of quadruples $(D+I)$, both decomposable D and indecomposable ones, and **b** dependence of the ratio I/D of the number of indecomposable I to the number of decomposable D quadruples, both as a function of the size of the polyene $N = 4\nu + 2$

8 Conclusions

Having established the linear dependence of the ratio I/D of the number of indecomposable I to the number of decomposable D singlet quadruples as a function of the size of the polyene $N = 2n = 4\nu + 2$ via direct evaluation of the number of respective clusters or CSFs, we recall [34] a qualitative reasoning that anticipates this result. Having n occupied and n unoccupied MOs, the number of singly-excited configurations scales as n^2 and the number of doubly-excited as n^4. The requirement of a zero overall quasimomentum reduces the n^4 dependence to n^3 [note that the available symmetries can only modify an overall numerical factor—e.g., when all the symmetries including the alternancy symmetry, are accounted for, the dependence is $n^3/6$—see also Eq. (29)]. Similarly, the number of quadruply-excited configurations will scale as n^8, and as n^7 when we impose the requirement of a zero quasimomentum. At the same time, the number of $\frac{1}{2}T_2^2$-type disconnected quadruples will vary only as $(n^3)^2 = n^6$, ignoring again the numerical factors due to various symmetries. Consequently, the dependence of the ratio of all quadruples to the number of decomposable ones, i.e., $(I + D)/D = I/D + 1$, on $N = 2n$ as $N \to \infty$ will be linear, since $n^7/n^6 = n$. This simple dimensional reasoning thus corroborates our results obtained by actual evaluation of the number of pertinent clusters. Clearly, the number of indecomposable quadruples will dominate the quadruply-excited manifold as $N \to \infty$. Yet, the actual role played by these clusters in the calculation of the exact correlation energy is not presently known and would deserve to be investigated.

The just outlined dimensional argument can now be extended to higher than quadruples. The number of $p(= 2t)$-times excited configurations scaling as n^{2p} is reduces to the $n^{2p-1} = n^{4t-1}$ dependence when we take into account the zero quasimomentum requirement. (Note that for the odd-number-of-times excited clusters, such as T_3, the role of connected and disconnected clusters is reversed, the latter ones being much less important than the former ones, not to mention the much smaller importance of even connected clusters of this type for the correlation energy, cf., e.g., Table 1; moreover, the T_1 clusters vanish entirely in view of the Brueckner character of the MOs). Next, the number of corresponding disconnected clusters constituting $(1/t!)T_2^t$ scales as $(n^3)^t$, so that the relevant ratio yields $n^{4t-1}/n^{3t} = n^{t-1} = n^{\frac{1}{2}p-1}$. Thus, for quadruples ($p = 4$), hexuples ($p = 6$), octuples ($p = 8$), etc., we find that the pertinent ratio I/D scales as n, n^2, n^3, etc., as $n \to \infty$, making the role of indecomposables even more important as the excitation order increases. This at least partially explains the difficulties of calculating the correlation energies for 1D extended systems as well as the complexity of the Bethe Ansatz wave functions. We recall that as one approaches the fully correlated limit ($\beta = 0$), all orbital energies become degenerate and thus all the configurations involved.

9 Summary

Relying on semi-empirical models of cyclic polyenes we have shown that within the CC description there exist two distinct types of connected, quadruply-excited clusters, which we designated as the *decomposable* and the *indecomposable* ones.

The indecomposable quadruples, in contrast to the ubiquitous decomposable ones, do not possess the corresponding disconnected counterparts given by the product of pair clusters. As we have pointed out, this phenomenon is associated with the high spatial symmetry of our model and cannot arise in asymmetric species. However, it will generally arise when handling low-dimensional extended systems, such as the one-dimensional (1D) or quasi-1D metals, 1D photonic crystals or polymeric chains with cyclic boundary conditions.

An account of quadruples is essential for a proper description of correlation effects. For most molecular systems, this may be efficiently achieved by exploiting the CCD (or CCSD) formalism (with an eventual perturbative correction for triples), in which case the quadruples are satisfactorily approximated by their disconnected component $\frac{1}{2}T_2^2$. However, there is no such possibility for indecomposable quadruples which have no disconnected counterparts. Moreover, as we have seen, their preponderance increases with the size of the linear chain. It would thus be useful to find out the role played by this type of clusters when accounting for the correlation effects in strongly correlated systems. In particular, it would be important to find out to what extent we can handle quadruples via the ACPQ-type approaches [34,64,66] that provide excellent results even for medium-sized systems (such as $C_{22}H_{22}$) in the entire range of the coupling constant and faithfully reproduce the exact correlation energy in the strongly correlated limit for the PPP and Hubbard models. Moreover, the role of even higher-than-quadruply-excited clusters may be of concern including their indecomposables. These and similar factors may render the standard CC-type approaches ineffectual in handling of degenerate strongly-correlated systems unless suitably modified as in the ACPQ case. A better understanding of the structure of the Bethe Ansatz wave functions could be certainly helpful in these efforts.

Acknowledgments Two of the authors (J.P. and T.S.) are greatly indebted to the Alexander von Humboldt Foundation for its kind support that enabled their stay at the Max-Planck-Institute for Astrophysics at Garching bei München in Germany and they thank the latter Institute for its hospitality during their stay. Their heartfelt thanks are also due to their host, Prof. Dr. Geerd H. F. Diercksen, for his kind advice and collaboration and for making their stay as pleasant and productive as possible.

References

1. R.J. Bartlett, in *Modern Electronic Structure Theory*, vol. 1, ed. by D.R. Yarkony (World Scientific, Singapore, 1995), pp. 1047–1131.
2. J. Paldus, X. Li, Adv. Chem. Phys. **110**, 1 (1999)
3. T.D. Crawford, H.F. Schaefer III, in *Reviews of Computational Chemistry*, vol. 14, ed. by K.B. Lipkowitz, D.B. Boyd (Wiley, New York, 2000), pp. 33–136
4. J. Paldus, in *Handbook of Molecular Physics and Quantum Chemistry, Part 3, Chap. 19*, vol. 2, ed. by S. Wilson (Wiley, Chichester, 2003), pp. 272–313.
5. R.J. Bartlett, M. Musiał, Rev. Mod. Phys. **79**, 291 (2007)
6. I. Shavitt, R.J. Bartlett, *Many-Body Methods in Chemistry and Physics: MBPT and Coupled-Cluster Theory* (Cambridge University Press, Cambridge, 2009)
7. P. Čársky, J. Paldus, J. Pittner (eds.), *Recent Progress in Coupled Cluster Methods: Theory and Applications* (Springer, Berlin, 2010)
8. J. Paldus, in *Theory and Applications of Computational Chemistry: The First Forty Years, Chap. 7*, ed. by C.E. Dykstra, G. Frenking, K.S. Kim, G.E. Scuseria (Elsevier, Amsterdam, 2005), pp. 115–147.

9. R.J. Bartlett, in *Theory and Applications of Computational Chemistry: The First Forty Years, Chap. 42*, ed. by C.E. Dykstra, G. Frenking, K.S. Kim, G.E. Scuseria (Elsevier, Amsterdam, 2005), pp. 1191–1221.
10. J. Paldus, J. Pittner, P. Čársky, in *Recent Progress in Coupled Cluster Methods: Theory and Applications, Chap. 17*, ed. by P. Čársky, J. Paldus, J. Pittner (Springer, Berlin, 2010), pp. 455–489
11. H.A. Bethe, Z. Phys. **71**, 205 (1931)
12. W. Heisenberg, Z. Phys. **49**, 619 (1928)
13. L. Hulthén, Arkiv. Mat. Astron. Fys. A **26**, 1 (1938)
14. M.T. Batchelor, Phys. Today **60**, 36 (2007)
15. E.H. Lieb, W. Liniger, Phys. Rev. **130**, 1605 (1963)
16. C.N. Yang, Phys. Rev. Lett. **19**, 1312 (1967)
17. E.H. Lieb, F.Y. Wu, Phys. Rev. Lett. **20**, 1445 (1968)
18. E.H. Lieb, F.Y. Wu, Phys. A **321**, 1 (2003)
19. R.J. Baxter, Ann. Phys. (N.Y.) 70, 193 (1972).
20. I. Bloch, Nat. Phys. **1**, 23 (2005)
21. Z. Bajnok, L. Šamaj, Acta Phys. Slov. **61**, 129 (2011). and references therein
22. E.H. Lieb, D.C. Mattis (eds.), *Mathematical Physics in One Dimension: Exactly Soluble Models of Interacting Particles* (Academic Press, New York, 1966)
23. R.J. Baxter, *Exactly Solved Models in Statistical Mechanics* (Academic Press, New york, 1982)
24. M. Gaudin, *La Fonction d'Onde de Bethe (Masson, Paris, 1983); English translation: The Bethe Wavefunction* (Cambridge University Press, Cambridge, 2014)
25. A. Montorsi (ed.), *The Hubbard Model: A Reprint Volume* (World Scientific, Singapore, 1992)
26. V.E. Korepin, N.M. Bogoliubov, A.G. Izergin, *Quantum Inverse Scattering Method and Correlation Functions* (Cambridge University Press, Cambridge, 1993)
27. D. Baeriswyl, D.K. Campbell, J.M.P. Carmelo, F. Guinea, E. Louis, *The Hubbard Model: Its Physics and Mathematical Physics* (Plenum Press, New York, 1995)
28. Z.N.C. Ha, *Quantum Many-Body Systems in One Dimension* (World Scientific, Singapore, 1996)
29. B. Sutherland, *Beautiful Models: 70 Years of Exactly Solved Quantum Many-Body Problems* (World Scientific, Singapore, 2004)
30. F.H.L. Essler, H. Frahm, F. Göhmann, A. Klümper, V.E. Korepin, *The One-Dimensionsl Hubbard Model* (Cambridge University Press, Cambridge, 2005)
31. K. Hashimoto, Int. J. Quantum Chem. **28**, 581 (1985)
32. P. Piecuch, J. Čížek, J. Paldus, Int. J. Quantum Chem. **42**, 165 (1992)
33. K. Hashimoto, J. Čížek, J. Paldus, Int. J. Quantum Chem. **34**, 407 (1988)
34. J. Paldus, M. Takahashi, R.W.H. Cho, Phys. Rev. B **30**, 4267 (1984)
35. R. Pauncz, J. de Heer, P.-O. Löwdin, J. Chem. Phys. **36**, 2247 (1962)
36. R. Pauncz, J. de Heer, P.-O. Löwdin, J. Chem. Phys. **36**, 2257 (1962)
37. J. de Heer, R. Pauncz, J. Mol. Spectr. **5**, 326 (1960)
38. R. Pauncz, *Alternant Molecular Orbital Method* (W. B. Saunders, Philadelphia, 1967)
39. G.L. Bendazzoli, S. Evangelisti, Chem. Phys. Lett. **185**, 125 (1991)
40. G.L. Bendazzoli, S. Evangelisti, L. Gagliardi, Int. J. Quantum Chem. **51**, 13 (1994)
41. S. Evangelisti, G.L. Bendazzoli, Chem. Phys. Lett. **196**, 511 (1992)
42. G.L. Bendazzoli, S. Evangelisti, Int. J. Quantum Chem. **66**, 397 (1998)
43. R. Podeszwa, S.A. Kucharski, L.Z. Stolarczyk, J. Chem. Phys. 116, 480 (2002)
44. J. Paldus, M.J. Boyle, Int. J. Quantum Chem. **22**, 1281 (1982)
45. J. Paldus, in *Theoretical Chemistry: Advances and Perspectives*, vol. 2, ed. by H. Eyring, D.J. Henderson (Academic Press, New York, 1976), pp. 131–290.
46. J. Paldus, in *Mathematical Frontiers in Computational Chemical Physics, IMA Series*, vol. 15, ed. by D.G. Truhlar (Springer, Berlin, 1988), pp. 262–299
47. R.G. Parr, *The Quantum Theory of Molecular Electronic Structure* (Benjamin, New York, 1963)
48. N. Mataga, K. Nishimoto, Z. Phys, Chem. **13**, 140 (1957)
49. J. Čížek, J. Paldus, I. Hubač, Int. J. Quantum Chem. Symp. **8**, 293 (1974)
50. Y. Ooshika, J. Phys. Soc. Jpn. **12**, 1246 (1957)
51. T. Murai, Progr. Theor. Phys. **27**, 899 (1962)
52. D. Cazes, L. Salem, C. Tric, J. Polymer Sci.:Part C, No. 29, pp. 109–118 (1970).
53. J. Hubbard, Proc. R. Soc. A **244**, 199 (1958)
54. M. Urban, J. Noga, S.J. Cole, R.J. Bartlett, J. Chem. Phys. **83**, 4041 (1985)

55. K. Raghavachari, G.W. Trucks, J.A. Pople, M. Head-Gordon, Chem. Phys. Lett. **157**, 479 (1989)
56. J. Čížek, J. Chem. Phys. **45**, 4256 (1966)
57. J. Čížek, Adv. Chem. Phys. **14**, 35 (1969)
58. J. Čížek, J. Paldus, Int. J. Quantum Chem. **5**, 359 (1971)
59. J. Paldus, J. Čížek, I. Shavitt, Phys. Rev. A **5**, 50 (1972)
60. J. Paldus, J. Čížek, Adv. Quantum Chem. **9**, 105 (1975)
61. P.E.S. Wormer, J. Paldus, Adv. Quantum Chem. **51**, 59 (2006)
62. J. Paldus, J. Chem. Phys. **67**, 303 (1977)
63. P. Piecuch, J. Paldus, Theor. Chim. Acta **78**, 65 (1990)
64. P. Piecuch, R. Toboła, J. Paldus, Phys. Rev. A **54**, 1210 (1996)
65. P. Piecuch, J. Paldus, Theor. Chim. Acta **83**, 69 (1992)
66. P. Piecuch, R. Toboła, J. Paldus, Int. J. Quantum Chem. **55**, 133 (1995)
67. A.E. Kondo, P. Piecuch, J. Paldus, J. Chem. Phys. **104**, 8566 (1996)
68. X. Li, J. Paldus, J. Chem. Phys. **101**, 8812 (1994)
69. B. Jeziorski, J. Paldus, P. Jankowski, Int. J. Quantum Chem. **56**, 129 (1995)
70. D.J. Thouless, in *The Quantum Mechanics of Many-Body Systems,* 2nd edn. (Academic, New York, 1972), p. 57 (p. 35 in the 1961, 1st edn.)
71. J.-M. Maillet, in *Quantum Spaces: Poincaré Seminar 2007, Progress in Mathematical Physics*, vol. 53, ed. by B. Duplantier, V. Rivasseau (Birkhäuser Verlag, Basel, 2007), pp. 161–201